

Effect of the Structure of Cobalt Nanocrystal Organization on the Collective Magnetic Properties

C. Petit, V. Russier, and M. P. Pileni*

LM2N, UMR CNRS 7070, Université P. et M. Curie Bât F, 4 Place Jussieu, 75005 Paris, France

Received: February 10, 2003; In Final Form: June 3, 2003

The magnetic properties of 8-nm cobalt nanocrystals that have been deposited on a highly oriented pyrolytic graphite substrate and either organized in lines or in the form of a film with local ordering are compared. Collective properties governed by dipolar interactions and due to the nanocrystal organization in lines are demonstrated.

PACS: 75.75.+a, 31.15.Ne, 81.16.Dn, 81.16.Rf

Because of their small size, nanocrystals generally exhibit properties that differ considerably from those of the bulk solid state.¹ Finely divided magnetic nanoparticles are desirable, because of their large domains of applications, especially for data storage devices and sensors,² and their original magnetic properties.³ In the past few years, several groups have succeeded in organizing magnetic nanocrystals in two-dimensional (2D) superlattices. The magnetic responses were explained via dipolar interactions.^{4–6} Chains of cobalt nanocrystals were also observed.⁷ However, no evidence was reported that concerned the influence of the nanocrystal organization on the magnetic properties. In this letter, magnetic properties are compared when the nanocrystals are either randomly dispersed on a graphite substrate (highly oriented pyrolytic graphite, HOPG) with local self-organization (2D) or oriented along lines (one dimensional, 1D). It is shown, both theoretically and experimentally, that there is a structural effect with the magnetic properties of lines made of cobalt nanocrystals. To our knowledge, this is the first example showing real collective magnetic properties that are due to organization of the nanocrystal.

Cobalt nanocrystals were produced and characterized as described in the work of Legrand et al.⁸ After the synthesis, coated cobalt nanocrystals 8 nm in size, with a size distribution of 14%, were dispersed in hexane and their concentration was fixed at 5×10^{-7} M. A HOPG substrate was deposited in the bottom of a cell that contained 200 μ L of solution. During the evaporation process at room temperature, a magnetic field (1 T) was applied or not. At the end of the process, in a magnetic field, the uncoalesced cobalt nanocrystals were arranged in chains along the direction of the field (see Figure 1A), whereas without the presence of an applied field, an isotropic monolayer with local organization (Figure 1B) was formed. The average interparticle distance was unchanged and was equal to 10 nm (from center to center). In both cases, the blocking temperature was 90 K, instead of 78 K for the same nanocrystals that were isolated in solution. This increase was due to the dipolar interaction⁴ and indicates that the effect was similar for both the chains and the 2D monolayers. Hence, because the same amount of nanocrystals was deposited on the substrate, it is possible to compare the magnetic behavior of aligned cobalt nanocrystals with those that form a monolayer.

The magnetic properties were determined using a SQUID magnetometer⁹ at a temperature of 3 K. When the nanocrystals were oriented along a given direction and the applied field was parallel to the long axis of the chains, the hysteresis loop was more square than that obtained for an isotropic monolayer (see Figure 2A), and the following characteristics were observed:

- (1) The reduced remanence increases, from 0.52 to 0.60;
- (2) The saturation magnetization (120 emu/g) does not change, although it is attained at 1 T instead of 1.5 T;
- (3) The coercivity slightly increases, from 0.13 T to 0.14 T.

In superlattice chains, with an applied field oriented parallel to the substrate, the magnetic response evolves when the field is perpendicular or parallel to the chain direction (see Figure 2B), which revealed the following observations:

- (1) The magnetization is smoother than that obtained when its orientation is parallel;
- (2) Saturation magnetization is not attained, even at 2.5 T, when its orientation is perpendicular;
- (3) Decreases in the reduced remanence and coercivity, to 0.25 and 0.10 T, respectively, are observed.

To quantify this effect, a ratio of the reduced remanence measured for an applied field perpendicular or parallel to the chains is defined: $\gamma' = (M_r/M_s)^\perp / (M_r/M_s)^\parallel$ and is equal to 0.42. In a 2D superlattice, no change is observed when the field is applied in various directions in the surface plane (the demagnetizing factor remains the same) and $\gamma' = 1$ (see Figure 2C).

To explain such a drastic change in magnetic properties, relative to the nanocrystal organization, a model that has been previously described for the collective behavior of a 2D assembly of cobalt nanocrystals^{10,11} is extended. In the case of the well-ordered monolayers, the precise structure of the lattice (square or hexagonal) has only a negligible role.¹¹ Here, the importance of the local structure of the film is investigated in a quite general way. Magnetization curves at $T = 0$ K are calculated and compared for a monolayer of spherical, single-domain particles whose locations are fixed on the surface. Three different structures are considered: (i) a well-ordered, square-lattice monolayer, which is chosen as a reference system; (ii) a monolayer of particles that is characterized by an isotropic disorder (hard-sphere-like distribution on the surface); and (iii) a chainlike structure of particles, oriented parallel to a given direction.

Cobalt nanocrystals are considered as monodisperse Stoner–Wolfarth particles. They are characterized by their bulk satura-

* Author to whom correspondence should be addressed. E-mail: Pileni@sri.jussieu.fr.

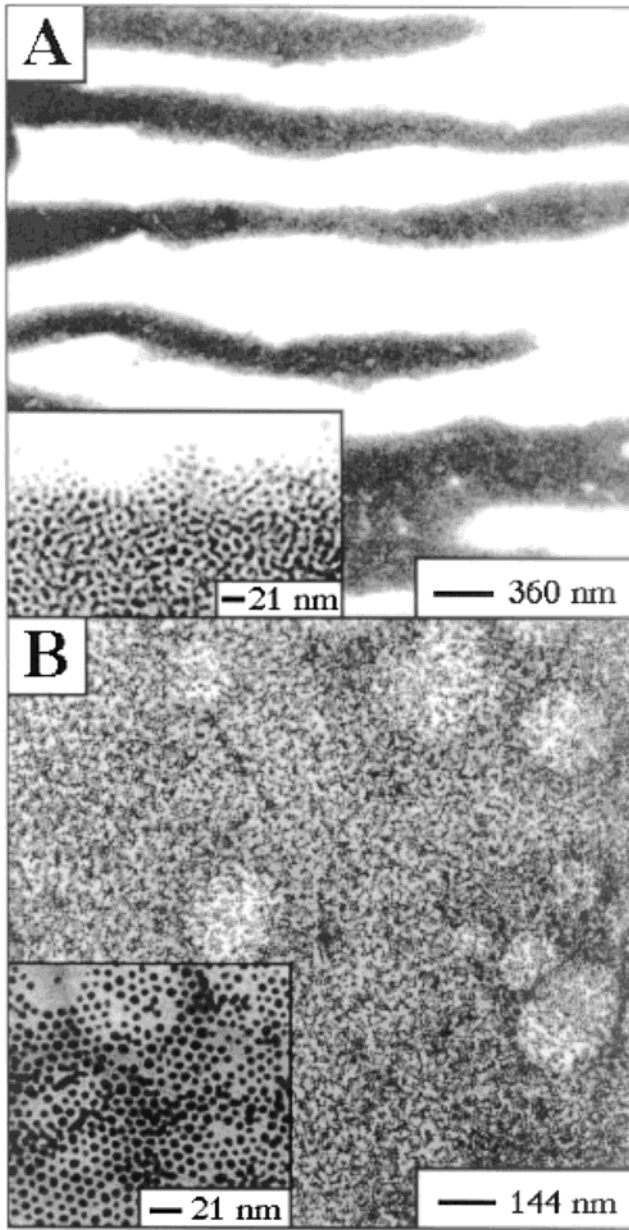


Figure 1. Low-magnification TEM images of 8-nm cobalt nanocrystals (A) organized in a linear structure by applying a magnetic field (1 T) parallel to the highly oriented pyrolytic graphite (HOPG) substrate during the evaporation process. (B) Partially organized in a two-dimensional (2D) monolayer on the substrate. Insets in each panel are higher-magnification views, showing the absence of coalescence or aggregation of the nanocrystals.

tion magnetization (M_s), their anisotropy constant (K), and their size (D). The particles are distributed on a plane surface with fixed positions and the easy-axes orientation ($\{\hat{n}_i\}$) are randomly distributed. Because a coating layer is present and protects the nanocrystals, there is no direct contact between neighboring nanocrystals. As a result, exchange interactions can be excluded and only dipolar interactions are considered. For a perfect square lattice, with a lattice spacing d , the influence of these interactions is characterized by the coupling constant: $\alpha_d = [\pi M_s^2 / (12K)](D/d)^3$, which is the ratio of the dipolar to the anisotropy energy. In the reference system, the nanocrystals occupy all the sites of a square lattice of length l , with $l^2/d^2 = n_s$ (n_s is the number of nanocrystals that are considered in the calculation). Details of the calculation were presented previously.¹¹ The surface plane is the (x, y) plane, and the z -axis is the normal to

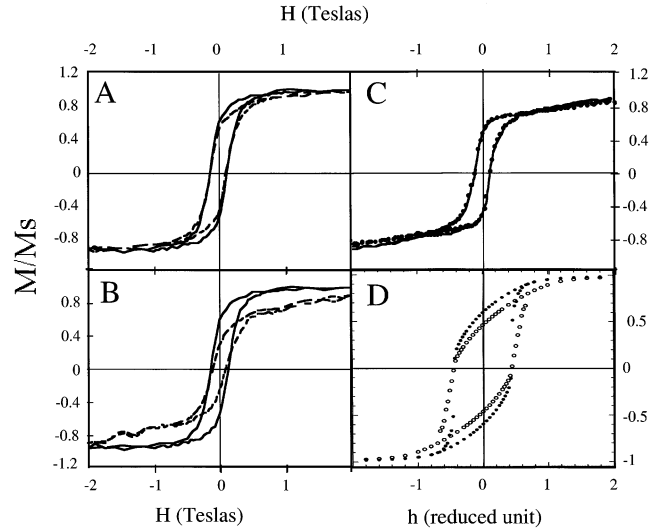


Figure 2. (A) Hysteresis curves, measured at 3 K, of (—) aligned and (---) partially disordered 8-nm cobalt nanocrystals. The applied field is oriented parallel to the substrate and along the direction of the particle orientation. (B) Hysteresis loop, measured at 3 K, when the applied field is oriented (—) parallel or (---) perpendicular to the nanocrystal orientation; the applied field is always oriented parallel to the substrate. (C) Hysteresis loop, measured at 3 K, for (—) the isotropic monolayer, compared to that of (●) the same sample turned 90°, always keeping the substrate parallel to the applied field. (D) Calculated magnetization curves for linear chains along the x -direction for $\alpha_d = 0.06$, with an applied field either (●) parallel or (○) normal to the direction of the chains, keeping the substrate parallel to the applied field.

the surface. Because of the vanishing temperature limit, the configuration of the moments ($\{\hat{\mu}\}$) is determined from the minimization of the total energy E . The total energy in reduced units, $E^* = E/(2K\nu_0)$, is given by

$$E^* = -\sum_i (\hat{n}_i \hat{\mu}_i)^2 - \frac{1}{2} \alpha_d \sum_{i \neq j} \frac{\hat{\mu}_i \hat{\mu}_j - 3(\hat{\mu}_i \hat{r}_{ij})(\hat{\mu}_j \hat{r}_{ij})}{(r_{ij}/d)^3} - h_a \sum_i \hat{\mu}_i \hat{h}_i \quad (1)$$

The calculation is performed for the 2D square box of finite size l , including n_s particles. Because of the long-range interaction, periodic boundary conditions in the two directions of the plane, x and y , are considered and the Ewald summation procedure is used. The calculated magnetization curve then corresponds to an infinite system that is composed of the periodically repeated unit cell including $n_s = 256$ particles. The number of chains in the box including the n_s particles that are explicitly considered in the calculation is not fixed but is related to their length and to the value of α_d^{eff} (see later discussion). In any case, for the densities considered here, the number of chains in the box does not influence the result of the calculation. The total energy is minimized, with respect to the $2n_s$ polar angles (θ_i, φ_i) of the moments from a conjugate gradient method. At each iteration of the numerical scheme, the energy is minimized along the calculated descent direction, using the Newton–Raphson method. To follow the hysteresis loop properly (metastable states), the variation of the angles at each iteration step is limited to $\delta\theta < \delta_m$, $\delta\varphi < \delta_m$, with $\delta_m \approx 0.2$. The reduced magnetization of the system in the direction of the field \hat{h} , $M(h_a)/M_s$, is then calculated.

In the two other cases, to estimate the influence of the structure on the magnetization curve, an effective coupling constant is introduced; it is calculated using the long-range

dependence and the anisotropy of the dipolar interactions. The effective coupling constant, α_d^{eff} , is determined and then the reference system that is characterized by the coupling constant, $\alpha_d = \alpha_d^{\text{eff}}$, is introduced. The hysteresis loop is modeled without any thermal effect ($T = 0$ K), because the experiments are performed at 3 K. The hysteresis loop is calculated in terms of the applied field $M_0(\alpha_d^{\text{eff}}, H)$ and is compared to that calculated for the real system, knowing the location of each nanocrystal in the film (2D-disordered or chainlike). From this difference, it is possible to evaluate the influence of local order in the layer on the magnetization curve of the system.

In the case of isotropic 2D monolayers, the effective coupling constant is determined only from the mean density of nanocrystals in the layer. The surface area occupation fraction (Φ) is the ratio of the surface area occupied by the nanocrystals ($n_s \pi D^2/4$) to that of the lattices (l^2): $\Phi = n_s \pi D^2/(4l^2)$. This determines the lattice spacing d_0 , which is the average distance between adjacent nanocrystals: $d_0/D = [\pi/(4\Phi)]^{1/2}$. The effective coupling constant then is

$$\alpha_d^{\text{eff}} = \frac{\pi M_s^2 (D)^3}{12K (d_0)^3} = \alpha_d^M \left(\frac{D}{d_0}\right)^3 \quad (2)$$

where α_d^M is the maximum value of the coupling constant. The parameter α_d^{eff} is used to calculate the magnetization of the reference system. The magnetization then is compared with the real case of the disordered monolayer. Here, we consider the special case of $\alpha_d^{\text{eff}} = 0.125$. This situation corresponds to 8-nm cobalt nanocrystals that are close-packed in a square lattice and represents the upper limit of our system. When the applied field is oriented parallel to the substrate (Figure 3A), there is almost no difference between the hysteresis loop of the square lattices (dashed line) and that of the real disordered system (data points). This is also true when the field is normal to the surface. The hysteresis loop is more square, with a reduced remanence, $M_r/M_s = 0.66$, than that calculated when the applied field is normal to the substrate, $M_r/M_s = 0.19$. As previously reported,¹⁰ the effect of the dipolar interactions is estimated, at a quantitative level, by the change in the reduced remanence magnetization M_r/M_s , at various α_d values, for the two orientations of the external applied field. The coupling constant α_d , which is deduced from the magnetic characterization of the 8-nm cobalt nanocrystals (with an anisotropy constant of 1.5×10^6 erg/cm³ and an average distance between nanocrystals of 9.8 nm), is equal to 0.06. The presence of holes and defects in the monolayers induces a decrease in this value to 0.05. From this value, the theoretical ratio, $\gamma_{\text{th}} = (M_r/M_s)^{\perp}/(M_r/M_s)^{\parallel}$, is 0.66. From the magnetization curves measured when the applied field is parallel and perpendicular to the substrate, the experimental value of γ is deduced and determined to be 0.65.¹⁰ There is good agreement between the theoretical value calculated on the reference model monolayer and the experimental data obtained when the nanocrystals are randomly dispersed on a substrate. Hence, it is shown that a well-ordered model is relevant to calculate the hysteresis curve of an isotropic disordered monolayer that is comprised of 8-nm cobalt nanocrystals, for any orientation of the applied field, relative to the substrate. The calculated magnetic properties are not dependent on the precise structure of the well-ordered monolayer. This is a consequence of the long-range dependence of the dipolar interaction.

For chainlike structures, to calculate α_d^{eff} , an intermediate step is first considered: a periodic arrangement of infinite parallel lines of nanocrystals at contact, parallel to the x -direction of the sample. This structure is considered to be a model lattice.

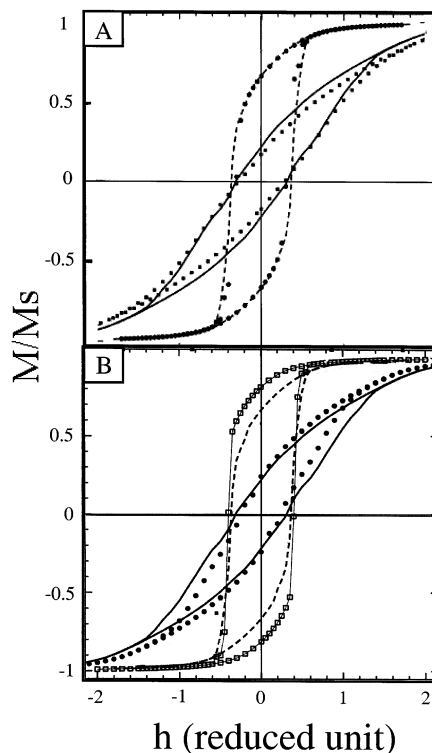


Figure 3. Hysteresis loop modeled for 8-nm cobalt nanocrystals with an effective coupling constant of 0.125: (A) magnetization of the real model for isotropic disorder (●) parallel to the plane and (■) perpendicular to the plane, and (B) magnetization of the real model for linear chains with the field oriented (□) collinear with the chain and (○) perpendicular to the chain. In each plot, the dotted and solid lines correspond to the perfect square model oriented parallel and perpendicular, respectively, to the substrate.

The distance between the lines of nanocrystals of diameter D is $a = [\pi/(4\Phi)]D$. The total dipolar interaction energy is estimated from the sum of the dipole–dipole energies in the two opposite cases, where all the particles have their moment oriented in the x - or z -direction (parallel to the chain and the surface or normal to the chain and the surface, respectively). The corresponding reduced sums are dependent only on $t = a/D$ and are given by the relations

$$S_x(t) = \sum_{m'} \frac{1 - 3(\hat{x}_{ij})^2}{(r_{ij}/D)^3}$$

$$S_z(t) = \sum_{m'} \frac{1}{(r_{ij}/D)^3} \quad (3)$$

where $\sum_{m'}$ denotes the sum over the sites of the model lattice, excluding $r_{ij} = 0$. When the moments are collinear with the x - or z -direction, the total dipolar energy can be written as

$$E_{dx}^m = \alpha_d^M \left(\frac{S_x(t)}{S_x^0} \right) S_x^0 \quad (\text{for the } x\text{-direction})$$

and

$$E_{dz}^m = \alpha_d^M \left(\frac{S_z(t)}{S_z^0} \right) S_z^0 \quad (\text{for the } z\text{-direction}) \quad (4)$$

where the terms $S_{x,z}^0$ are relative to a perfect square lattice ($t = 1$). An orientation-dependent, effective coupling constant can

be defined, in such a way that $E_{dx,z}^{*m} = E_{dx,z}^{*0}(\alpha_d^{\text{eff}})$. Finally, the effective coupling constant α_d^{eff} is defined as a mean value over the orientations in the x - and z -directions:

$$\alpha_d^{\text{eff}} = \frac{1}{2} \alpha_d^M \left(\frac{S_x(t)}{S_x^0} + \frac{S_z(t)}{S_z^0} \right) \quad (\text{with } t = a/D = \pi/(4\phi)) \quad (5)$$

The calculations are performed for both types of structures: square lattice (reference model), with an applied field oriented parallel or normal to the surface, and chainlike (real model), with an applied field in the surface plane and oriented parallel or perpendicular to the chains or perpendicular to the surface plane. The results of the calculations for the reference and real systems are then compared in the case of an effective coupling constant of $\alpha_d^{\text{eff}} = 0.125$ (see Figure 3B). There is a marked difference between the hysteresis loop of the square lattices (the dashed lines in Figure 3B) with the effective coupling constant and that of the linear chain system (the solid lines in Figure 3B) when the applied field is oriented parallel to the chains. A large increase in the reduced remanence is obtained ($M_r/M_s = 0.81$), compared to the reference system ($M_r/M_s = 0.66$), and the coercivity increases slightly. Applying the field perpendicular to the substrate leads to a smoother hysteresis loop, with a large decrease in the reduced remanence ($M_r/M_s = 0.20$). In this case, the coercivity decreases slightly (see Figure 3B). Contrary to the case where the field is parallel to the chains, the hysteresis loop calculated with the field oriented perpendicular to the substrate (and, accordingly, also perpendicular to the chains) agrees well with that of the reference model. Indeed, because of the dipolar coupling, the linear chains behave approximately as homogeneous wires with an effective easy axis in the direction of the chains, although individual nanocrystals have randomly distributed easy axes. The observed difference corresponds, to a first approximation, to the different orientations of the effective easy axes (parallel or perpendicular) of the wire, with respect to the applied field. Hence, it is shown that, theoretically, because of the structure, a well-ordered reference model is not relevant for calculating the hysteresis curve of linear chains. This implies that an exact calculation with the real model is necessary to determine the hysteresis loop of a network of linear chains oriented parallel or perpendicular to the measuring field, the latter being in the substrate plane. This has been done for a coupling constant of $\alpha_d = 0.06$, corresponding to the experimental case (see Figure 2D). The strength of the structural effect is estimated theoretically by comparing the reduced remanence in two geometries: either parallel or perpendicular to the chains, keeping the plane parallel to the applied field. A theoretical ratio, $\gamma'_{\text{th}} = (M_r/M_s)^{\perp}/(M_r/M_s)^{\parallel}$, is then deduced for the linear chains that are oriented in the x -direction from the two calculations, corresponding to $h = y$ and $h = x$, respectively (see Figure 2D). This is compared to the experimental value (see Figure 2B), to check the magnitude of this structural effect on the collective magnetic properties of the cobalt nanocrystals chains. The γ' values obtained from experiment (0.42) and from theory (0.77) have the same order of magnitude. For this coupling strength, no change in the coercivity can be observed theoretically. This is in relatively good agreement, at a qualitative level, with the results of the model that has been presented previously. Therefore, the deviation of γ' from a value of 1 can be attributed to the modification of the structure. Our systems are not the perfect linear chains as introduced in the theoretical

model. The experimental chains are larger than those in the theoretical model, and there are many bilayers in some regions of these chains (see Figure 1A). This, as well as the size polydispersity, probably explains the difference in magnitude between experiment and theory, both for the remanence and the coercivity. This collective effect does not suppose, as specified theoretically, an alignment of the easy axes of the nanocrystals that form the chains. It results only from the long-range dipolar interaction between the nanocrystals inside the chains. The chains behave approximately as a wire with an effective easy axis in the direction of the wire, and we found the same behavior as that observed in a homogeneous cylinder that was made of iron or cobalt.^{12,13} In fact, similar results have been observed recently for ferrite nanoparticles that were arranged in a tubelike structure, where it has been demonstrated that the easy axes were not aligned.¹⁴ However, an effect of the alignment of the easy axes during the deposition in a field cannot be totally excluded and could also explain the discrepancy between theory and experiment. Indeed, the results reported above seem to be mainly a structural effect on the collective magnetic properties in the 1D chains that are made of non-coalesced cobalt nanocrystals, as predicted theoretically.

To summarize, cobalt nanocrystals with an average diameter of 8 nm can form monolayers with local order. Because of the long-range scale of dipolar interactions, the collective magnetic properties are not dependent on the level of order inside the monolayer. Conversely, when cobalt nanocrystals are aligned, the collective magnetic properties are dependent on the structure of the organization, and these chains of nanocrystals behave approximately as nanowires.

Acknowledgment. We are grateful to Dr. Eric Vincent of DSM–DRECAM–SPEC for fruitful discussions and to Dr. G. Lebras and L. Lepape for provision of the SQUID equipment.

References and Notes

- (1) Feldheim, D. L.; Foss, C. A., Jr., Eds. *Metal Nanoparticles: Synthesis, Characterization, and Applications*; Marcel Dekker: New York, 2002.
- (2) Sellmyer, D. J.; Yu, M.; Kirby, R. D. *Nanostruct. Mater.* **1999**, *12*, 1021.
- (3) Dormann, J. L.; Fiorani, D.; Tronc, E. In *Advances in Chemical Physics*; Prigogine, I., Rice, S. A., Eds.; Wiley: New York, 1997; Vol. XCVIII.
- (4) Petit, C.; Taleb, A.; Pileni, M. P. *Adv. Mater.* **1998**, *10*, 259; *J. Phys. Chem. B* **1999**, *103*, 1805.
- (5) Ngo, A.; Pileni, M. P. *Adv. Mater.* **2000**, *12*, 276; *J. Phys. Chem.* **2001**, *105*, 53.
- (6) Sun, S.; Murray, C. B. *J. Appl. Phys.* **1999**, *85*, 4235.
- (7) Wiedwald, U.; Spasova, M.; Farle, M.; Hilgendorff, M.; Giersig, M. *J. Vac. Sci. Technol. A* **2001**, *19*, 1773.
- (8) Legrand, J.; Petit, C.; Pileni, M. P. *J. Phys. Chem. B* **2001**, *105*, 5643.
- (9) Magnetic measurements were made with a Cryogenic S600 SQUID magnetometer. To avoid artifacts due to the magnetic history of the sample, the sample was always removed from the magnetometer, to change its orientation at room temperature (far away from its blocking temperature (90 K)). After few minutes, the sample was then cooled to 3 K and the magnetic field finally was applied. The parallel measurement was performed first.
- (10) Russier, V.; Petit, C.; Legrand, J.; Pileni, M. P. *Phys. Rev. B* **2000**, *62*, 3910.
- (11) Russier, V. *J. Appl. Phys.* **2001**, *89*, 1287.
- (12) Encinas-Oropesa, A.; Demand, M.; Pinaux, L.; Ebels, U.; Huynen, I. *J. Appl. Phys.* **2001**, *89*, 6704.
- (13) Henry, Y.; Ounadjela, K.; Piraux, L.; Dubois, S.; George, J.-M.; Duval, J.-L. *Eur. Phys. J. B* **2001**, *20*, 35.
- (14) Lalatonne, Y.; Motte, L.; Russier, V.; Ngo, A. T.; Bonville, P.; Pileni, M. P., submitted for publication.